Distorted-wave impulse-approximation calculations for quasifree cluster knockout reactions*

N. S. Chant and P. G. Roos
Department of Physics and Astronomy, University of Maryland, College Park, Maryland 20742
(Received 30 August 1976)

A formalism for distorted-wave impulse-approximation calculations of quasifree cluster knockout reactions is described. Results are presented for $(p,p\alpha)$ and $(\alpha,2\alpha)$ reactions. In both cases distortion effects are large. It is concluded that incident energies between ~ 100 and ~ 200 MeV are most suitable for $(p,p\alpha)$ studies of nuclear structure, whereas somewhat higher energies are more appropriate for $(\alpha,2\alpha)$ studies.

[NUCLEAR REACTIONS DWIA reaction theory of cluster knockout.]

I. INTRODUCTION

Studies of quasifree cluster knockout reactions such as $(p,p\alpha)$ can, in principle, provide quite precise information concerning clustering effects in nuclei.[1] Such studies tend to emphasize low momentum components of the ejected cluster wave function and thus complement studies of cluster transfer processes[2] such as (^{3}He, ^{7}Be) which tend to probe higher momentum components of the cluster wave function. Evidently a prerequisite of this type of investigation is a good understanding of the reaction mechanism so that the transition amplitude may be separated (perhaps somewhat artificially) into a reaction term and a nuclear structure term. In the case of transfer processes many successful distorted-wave Born-approximation calculations have been reported[3] which appear to provide reliable tests of nuclear structure calculations. For knockout processes distorted-wave impulse-approximation (DWIA) calculations have been reported[4-6] mostly for nucleon removal experiments. We are aware of only a small number of DWIA calculations for the removal of two or more nucleons,[7,8] and these have been restricted to cases where no angular momentum transfer occurs. In general, analyses of cluster knockout reactions have used some form of plane-wave impulse-approximation analysis (PWIA). Frequently it has been necessary to introduce a radial cutoff parameter in order to simulate the effects of distortion of the incident and emitted particle wave functions by the residual nucleus. Such an arbitrary procedure raises doubts as to the validity of the resultant nuclear structure information. Evidently, cluster knockout reactions are in much the same situation now as were transfer reactions in the early 1960's. At that time only a few distorted-wave calculations were available and most experiments were analyzed using Butler theory, a simple plane-wave calculation employing a radial cutoff.

In view of the improved precision of current cluster knockout data[1] a proper treatment of distortion effects is essential to the utilization of this reaction for spectroscopic studies. In the present paper we wish to describe a general DWIA code for nucleon and cluster knockout. This code is used to investigate the effects of distortion in a few typical experiments and to predict certain features of cluster knockout which have not so far been studied. Some limited applications to specific data for α cluster removal are also presented.

II. THE CALCULATION

In the following discussion we follow closely the work of Berggren and Jackson,[4] and of Lim and McCarthy[5] for nucleon knockout. The generalization to cluster knockout is rather straightforward.

A. Formulation

Let us consider a cluster knockout reaction $A(a,a'b)B$ where the emitted cluster is b so that $A = B + b$ and where the $'$ serves to identify particle a in the exit channel. For this reaction the differential cross section is given by

$$\sigma_{BA} = \frac{2\pi}{\hbar v} |T_{BA}|^2 \omega_B \ , \tag{1}$$

where v is the relative velocity of a and A in the entrance channel and ω_B is the energy density of final states. The reduced transition amplitude[9] T_{BA} is given by

$$T_{BA} = \langle \Phi^{(-)}(\widetilde{B,a',b}) | V_{ba} | \Psi^{(+)}(\widetilde{A,a}) \rangle \ , \tag{2}$$

where $\Psi^{(+)}$ is the exact wave function for the system and $\Phi^{(-)}$ is the solution (with ingoing wave boundary conditions) obtained when the potential V_{ba}, acting between the particles b and a in the exit channel, is neglected. The $\sim$ serves as a re-

minder that both wave functions are antisymmetric with respect to interchange of any two nucleons. Introducing $\Phi^{(+)}(\widetilde{A,a})$, the wave function for the entrance channel in the absence of V_{ba}, we can define a t operator so that

$$T_{BA} = \langle \Phi^{(-)}(\widetilde{B,a',b}) | t_{BA} | \Phi^{(+)}(\widetilde{A,a}) \rangle \ . \tag{3}$$

We next express the wave functions in Eq. (3) in terms of products of separately antisymmetrized wave functions. The result, provided terms in which nucleons are exchanged between the projectile a and the residual nucleus B are neglected, is of the following form:

$$T_{BA} = (A!/B!b!)^{1/2} \langle \Phi(\tilde{B}) \Phi(\widetilde{a',b}) | t_{BA} | \mathcal{A}_{ab} \Phi(\tilde{A}) \Phi(\tilde{a}) \rangle \ , \tag{4}$$

where the wave function for particle K is $\Phi(\tilde{K})$. The operator $\mathcal{A}_{ab}$ is an antisymmetrizer between nucleons in the projectile and the b "extra-core" nucleons which are ejected. Finally, $\Phi(\widetilde{a',b})$ is a properly antisymmetrized product of functions given by

$$\Phi(\widetilde{a',b}) = \mathcal{A}_{ab} \{ \Phi(\tilde{a}) \Phi(\tilde{b}) \} \ . \tag{5}$$

Now, writing out the wave functions in more detail,

$$T_{BA} = (A!/B!b!)^{1/2} \langle \Psi_{J_B M_B T_B N_B}(\tilde{B}) \mathcal{A}_{ab} \eta^{(-)}_{Bab} \Psi_{s_a \sigma'_a t_a \nu_a}(\tilde{a}) \Psi_{s_b \sigma'_b t_b \nu_b}(\tilde{b}) | t_{BA} | \mathcal{A}_{ab} \eta^{(+)}_{Aa} \Psi_{J_A M_A T_A N_A}(\tilde{A}) \Psi_{s_a \sigma_a t_a \nu_a}(\tilde{a}) \rangle \ , \tag{6}$$

where the Ψ are internal wave functions for the various particles and $\eta^{(+)}_{Aa}$ and $\eta^{(-)}_{Bab}$ describe the relative motion of the mass centers of the particles in the entrance and exit channels, respectively. The angular momentum and isospin quantum numbers for the target are J_A (projection M_A) and T_A (projection N_A), respectively. Similarly, the corresponding quantities for the projectile are $s_a(\sigma_a)$ and $t_a(\nu_a)$. The quantum numbers for the emitted particles are defined similarly.

At this point we are in a position to integrate over the internal coordinates of the residual nucleus provided that t_{BA} is assumed not to act upon these variables. Evidently the result of projecting the target nucleus A onto the residual nucleus B is a complicated function of the coordinates of the remaining b nucleons. In order to simplify matters somewhat, we assume that these nucleons contribute significantly to the cross section only when their relative motion and spin-isospin wave function is identical to that in the emitted cluster b. Thus, projecting out this wave function, which we denote by $\Psi_{s_b \sigma_b t_b \nu_b}(\tilde{b})$, and at the same time integrating over the internal coordinates of B, we can write

$$T_{BA} = (A!/B!b!)^{1/2} \sum_{\alpha L J \sigma_b \Lambda M} g_{AB}(\alpha L s_b J t_b)(t_b \nu_b T_B N_B | T_A N_A)(JM J_B M_B | J_A M_A)(L \Lambda s_b \sigma_b | JM)$$
$$\times \langle \mathcal{A}_{ab} \eta^{(-)}_{Bab} \Psi_{s_a \sigma'_a t_a \nu_a}(\tilde{a}) \Psi_{s_b \sigma'_b t_b \nu_b}(\tilde{b}) | t_{BA} | \mathcal{A}_{ab} \eta^{(+)}_{Aa} \phi^{\alpha}_{L\Lambda}(\vec{r}_{bB}) \Psi_{s_a \sigma_a t_a \nu_a}(\tilde{a}) \Psi_{s_b \sigma_b t_b \nu_b}(\tilde{b}) \rangle \ , \tag{7}$$

where

$$\langle \Psi_{J_B M_B T_B N_B}(\tilde{B}) \Psi_{s_b \sigma_b t_b \nu_b}(\tilde{b}) | \Psi_{J_A M_A T_A N_A}(\tilde{A}) \rangle = \sum_{\alpha L J \sigma_b \Lambda M} g_{AB}(\alpha L s_b J t_b)(t_b \nu_b T_B N_B | T_A N_A)(JM J_B M_B | J_A M_A)$$
$$\times (L \Lambda s_b \sigma_b | JM) \phi^{\alpha}_{L\Lambda}(\vec{r}_{bB}) \ , \tag{8}$$

where $\phi^{\alpha}_{L\Lambda}(\vec{r}_{bB})$ describes the motion of the c.m. of b with respect to the c.m. of B and is normalized to unity. The relative angular momentum of b and B is L (projection Λ), and any other quantum numbers needed to specify the motion are denoted by α. Equation (8) can be regarded as defining the "cluster coefficient of fractional parentage," $g_{AB}(\alpha LSJT)$.

We now introduce the impulse approximation, which is to replace t_{BA} by the two-body operator for the free $a+b$ scattering process $t^{(+)}_f$. Noticing that the operator $\mathcal{A}_{ab}$ acting upon the wave functions to its right yields the antisymmetrized product $\Phi_{s_a \sigma_a s_b \sigma_b t_a \nu_a t_b \nu_b}(\widetilde{a,b})$, and employing expansions of the relative motion wave functions in momentum space, it is possible to isolate the matrix elements of $t^{(+)}_f$. Introducing the additional assumption that the resultant reduced t matrix varies sufficiently slowly with momenta that its arguments may be replaced by their asymptotic values, we obtain a factorized form for T_{BA}. As is well known, this procedure leads to a convenient zero range expression. The result is

$$T_{BA} = (A!/B!b!)^{1/2} \sum_{\alpha L J \sigma_b \Lambda M} g_{AB}(\alpha L s_b J t_b)(t_b \nu_b T_B N_B | T_A N_A)(JM J_B M_B | J_A M_A)(L \Lambda s_b \sigma_b | JM) \langle \vec{k}_{f'} \sigma'_a \sigma'_b | t^{(+)}_f | \vec{k}_{i'} \sigma_{a'} \sigma_b \rangle$$
$$\times \langle \eta^{(-)}_{Bab} | \delta(\vec{r}_a - \vec{r}_b) | \eta^{(+)}_{Aa} \phi^{\alpha}_{L\Lambda}(\vec{r}_{bB}) \rangle \ , \tag{9}$$

where $\vec{k}_i$ and $\vec{k}_f$ are the initial and final relative momenta of particles a and b, and where for brevity we have retained only spin projection quantum numbers in writing the two-body reduced t matrix. Now writing

$$S_{\alpha LJ}^{1/2} = (A!/B!b!)^{1/2} g_{AB}(\alpha L s_b J t_b) , \tag{10}$$

$$T_{BA}^{\alpha L\Lambda} = (2L+1)^{-1/2} \langle \eta_{Bab}^{(-)} | \delta(\vec{r}_a - \vec{r}_b) | \eta_{Aa}^{(+)} \phi_{L\Lambda}^{\alpha}(\vec{r}_{bB}) \rangle , \tag{11}$$

and denoting the isospin coupling coefficient $(t_b \nu_b T_B N_B | T_A N_A)$ by C, we have

$$T_{BA} = C \sum_{\alpha LJ\Lambda M\sigma_b} S_{\alpha LJ}{}^{1/2} (JM J_B M_B | J_A M_A)(L\Lambda s_b \sigma_b | JM)(2L+1)^{1/2} T_{BA}^{\alpha L\Lambda} \langle \vec{k}_f, \sigma_a, \sigma_b' | t_f^{(+)} | \vec{k}_i, \sigma_a, \sigma_b \rangle . \tag{12}$$

Inserting Eq. (12) into Eq. (1), averaging over M_A and σ_a, and summing over M_B, σ_a' and σ_b', we obtain

$$\sigma_{BA} = \frac{2\pi}{\hbar v} \omega_B C^2 \sum_{\sigma_a \sigma_a' \sigma_b' J M} \frac{1}{(2J_A+1)(2s_a+1)} \left| \sum_{\alpha L\Lambda\sigma_b} S_{\alpha LJ}{}^{1/2} (L\Lambda s_b \sigma_b | JM)(2L+1)^{1/2} \right.$$
$$\left. \times T_{BA}^{\alpha L\Lambda} \langle \vec{k}_f, \sigma_a', \sigma_b' | t_f^{(+)} | \vec{k}_i, \sigma_a, \sigma_b \rangle \right|^2 . \tag{13}$$

Notice that, in general, the summation over the orbital angular momentum transfer $L\Lambda$ is coherent despite the omission of spin dependent distortions in evaluating $T_{BA}^{\alpha L\Lambda}$. Furthermore, even if the additional assumption is made that the two-body t matrix is independent of σ_b, the coherence between different values of L and Λ persists. Nevertheless, in many cases of interest further simplication of Eq. (13) is possible. Thus we may write

$$\sigma_{BA} = \frac{2\pi}{\hbar v} \omega_B C^2 |\overline{\langle t \rangle}|^2 \sum_{LJ\Lambda} \left| \sum_{\alpha} S_{\alpha LJ}{}^{1/2} T_{BA}^{\alpha L\Lambda} \right|^2 , \tag{14}$$

where

$$|\overline{\langle t \rangle}|^2 = \frac{1}{(2s_a+1)(2s_b+1)} \sum_{\sigma_a \sigma_b \sigma_a' \sigma_b'} |\langle \vec{k}_f, \sigma_a', \sigma_b' | t_f^{(+)} | \vec{k}_i, \sigma_a, \sigma_b \rangle|^2 \tag{15}$$

is the square of the two-body matrix averaged over initial spin projections and summed over final spin projections. The expression given in Eq. (14) is exact provided $s_b = 0$, $L = 0$, or $s_b = \frac{1}{2}$. The first two cases are obvious by inspection of Eq. (13). For $s_b = \frac{1}{2}$ it may be shown that the form of the result is a consequence of parity conservation.[10] Notice that if the additional quantum numbers α are not needed, or if $T_{BA}^{\alpha L\Lambda}$ is independent of α, we can define a spectroscopic factor

$$S_{LJ} = \left| \sum_{\alpha} S_{\alpha LJ}{}^{1/2} \right|^2 , \tag{16}$$

and for specific values of L and J

$$\sigma_{BA}^{LJ} = \frac{2\pi}{\hbar v} \omega_B C^2 |\overline{\langle t \rangle}|^2 S_{LJ} \sum_{\Lambda} \left| T_{BA}^{\alpha L\Lambda} \right|^2 . \tag{17}$$

In the cases where Eq. (17) is appropriate, the spectroscopic factor S_{LJ} can be omitted from the calculation and determined empirically by normalization to experiment. On the other hand, the use of Eqs. (13) or (14) necessitates prior knowledge of the spectroscopic amplitudes $S_{\alpha LJ}{}^{1/2}$, which must be taken from some theoretical calculation. In order to clarify the use of such amplitudes and the comparison of empirical spectroscopic factors with theory, we here restate the definitions implicitly contained in Eqs. (8) and (10).

Inverting Eq. (8), we find

$$C S_{\alpha LJ}{}^{1/2} = (A!/B!b!)^{1/2} \sum_{\Lambda\sigma_b M M_B} (L\Lambda s_b \sigma_b | JM)(JM J_B M_B | J_A M_A)$$
$$\times \langle \Psi_{J_B M_B T_B N_B}(\tilde{B}) \Psi_{s_b \sigma_b t_b \nu_b}(\tilde{b}) \phi_{L\Lambda}^{\alpha}(\vec{r}_{bB}) | \Psi_{J_A M_A T_A N_A}(\tilde{A}) \rangle . \tag{18}$$

Comparison with Eq. (III.56) of Ref. 11 shows that when b is a nucleon $(S_{\alpha LJ}{}^{1/2})^2$ is simply the usual stripping or pickup spectroscopic factor. Similarly, for α particle knockout Eq. (18) reduces to Eq. (5.11) of Ichimura *et al.*,[12] so that $S_{\alpha LJ}{}^{1/2}$ is identical to the quantity $A_{Nl}(A,A')$ of that paper. From the discussion of Ref. 12 it is straightforward to obtain the expression given for the spectroscopic factor S by Kurath[13] in his tabulation of α structure amplitudes for the $1p$ shell. The result is $S = |A_{Nl}(A,A')|^2$ so that Kurath's spectroscopic factor is our quantity S_{LJ} defined in Eq. (16). Finally we note that, apart from a possible phase difference, our amplitude $S_{\alpha LJ}{}^{1/2}$ is identi-

cal to the generalized k-nucleon spectroscopic amplitude $\theta(LS_kT_kJ)$ defined in Eq. (5.5) of the paper by Anyas Weiss *et al.*[14]

B. Evaluation of the amplitude $T_{BA}^{\alpha L\Lambda}$

Following closely the discussion of Ref. 4, we write the Hamiltonian for the system as

$$H = H_a + H_A + T_a + T_A + V_{aA} \quad \text{(entrance channel)} , \tag{19}$$

$$H = H_a + H_b + H_B + T_a + T_b + T_B + V_{ab} + V_{bB} + V_{aB} \quad \text{(exit channel)}, \tag{20}$$

where H_i and T_i are, respectively, the internal Hamiltonian and the kinetic energy operator for particle i. As pointed out earlier, the initial and final scattering states are generated using $H' = H - V_{ab}$. As shown in Ref. 4, it is possible to reexpress the kinetic energy operators occurring in Eq. (19) in terms of the overall c.m. kinetic energy and a term T_{aA} involving the square of the momentum operator conjugate to $\vec{r}_{aA}$.

Thus $\eta_{Aa}^{(+)}$ satisfies

$$(T_{aA} + V_{aA} - V_{ab} + \epsilon_{aA})\eta_{Aa}^{(+)} = 0 , \tag{21}$$

where ϵ_{aA} is the relative kinetic energy and $T_{aA} = (-\hbar^2\nabla_{aA}^2)/2\mu_{aA}$, where μ_{ij} is the reduced mass of particles i and j. In the calculations which follow we take $V_{aA} - V_{ab} \simeq V_{aB}(\vec{r}_{aA})$, the optical potential for $a+B$ scattering averaged in some sense over the target nucleus A. This point is discussed further in Ref. 4. We hope that, in general, this potential will differ little from the optical potential for $a+A$ scattering.

For the exit channel scattering solution we eliminate the c.m. kinetic energy and reexpress the Hamiltonian in terms of the momentum operators conjugate to $\vec{r}_{aB}$ and $\vec{r}_{bB}$. The result is

$$H - V_{ab} - T^{\text{c.m.}} = H_a + H_b + H_B + T_{aB} + T_{bB} + V_{aB} + V_{bB} + T_{\text{coup}} , \tag{22}$$

where $T^{\text{c.m.}}$ is the c.m. kinetic energy term and

$$T_{\text{coup}} = -\hbar^2 \frac{\nabla_{aB} \cdot \nabla_{bB}}{m_B} . \tag{23}$$

Clearly this term should have little effect, provided $m_B \ll \mu_{aB}$ and/or $m_B \ll \mu_{bB}$. If it is neglected, the exit channel scattering state factorizes

$$\eta_{Bab}^{(-)} = \chi_{aB}^{(-)}(\vec{k}_{aB}, \vec{r}_{aB})\chi_{bB}^{(-)}(\vec{k}_{bB}, \vec{r}_{bB}) , \tag{24}$$

where

$$(T_{aB} + V_{aB} - \epsilon_{aB})\chi_{aB}^{(-)}(\vec{k}_{aB}, \vec{r}_{aB}) = 0 \tag{25}$$

and

$$(T_{bB} + V_{bB} - \epsilon_{bB})\chi_{bB}^{(-)}(\vec{k}_{bB}, \vec{r}_{bB}) = 0 . \tag{26}$$

The potentials V_{aB} and V_{bB} are taken to be the optical potentials which describe the $a+B$ and $b+B$ scattering at the relative energies ϵ_{aB} and ϵ_{bB}, respectively. These relative energies, as well as ϵ_{aA} in Eq. (21), are defined by

$$\begin{aligned} \epsilon_{aB} &= P_{AB}^2/2\mu_{aB} , \\ \epsilon_{bB} &= P_{bB}^2/2\mu_{bB} , \\ \epsilon_{aA} &= P_{aA}^2/2\mu_{aA} , \end{aligned} \tag{27}$$

where

$$\begin{aligned} \vec{P}_{aA} &= \frac{A}{A+a}\vec{P}_a , \\ \vec{P}_{aB} &= \vec{P}_a' - \frac{a}{a+b+B}\vec{P}_a , \\ \vec{P}_{bB} &= \vec{P}_b - \frac{b}{a+b+B}\vec{P}_a \end{aligned} \tag{28}$$

and $\vec{P}_a$, $\vec{P}_a'$, $\vec{P}_b$, and $\vec{P}_B$ are the laboratory momenta for the incident particle and the three emitted particles. These momenta are generated relativistically in our calculations. Notice that our choices for ϵ_{aB} and ϵ_{bB} correspond to replacing the operator T_{coup} by $\vec{P}_{aB} \cdot \vec{P}_{bB}/m_B$, its contribution to the overall energy eigenvalue, and lead to correct asymptotic momenta. Thus Eq. (27) is equivalent to Koshel's nonstatic approximation[15] and, in addition, yields the correct plane-wave limit.

In order to evaluate Eq. (11) for $T_{BA}^{\alpha L\Lambda}$ it remains to generate the function $\phi_{L\Lambda}^{\alpha}(\vec{r}_{bB})$. Strictly, this results from projecting the many-body wave function for A onto the residual nuclei B and b. Such a procedure is beyond the scope of the present work. Rather, we simply introduce a phenomenological real (Woods-Saxon) potential V_{WS} which is adjusted to reproduce the empirical $A \to B + b$ separation energy S_{Bb}:

$$(T_{bB} + V_{\text{WS}} - S_{Bb})\phi_{L\Lambda}^{\alpha}(\vec{r}_{bB}) = 0 . \tag{29}$$

Substituting for $\eta_{Aa}^{(+)}$ and $\eta_{Bab}^{(-)}$ in Eq. (11) and integrating over $\vec{r}_{ab}$ we obtain

$$T_{BA}^{\alpha L\Lambda} = \frac{1}{(2L+1)^{1/2}} \int \chi_{aB}^{(-)*}(\vec{k}_{aB}, \vec{r})\chi_{bB}^{(-)*}(\vec{k}_{bB}, \vec{r}) \times \chi_{aA}^{(+)}(\vec{k}_{aA}, \gamma\vec{r})\phi_{L\Lambda}^{\alpha}(\vec{r})d\vec{r} , \tag{30}$$

where we have made use of the relationships

$$\begin{aligned} \vec{r}_{aB} &= \vec{r}_{ab} + \vec{r}_{bB} , \\ \vec{r}_{aA} &= \vec{r}_{ab} + \gamma\vec{r}_{bB} , \end{aligned} \tag{31}$$

and

$$\gamma = B/(B+b) .$$

To proceed further we make partial wave expansions

$$\chi^{(+)}_{aA}(\vec{k}_{aA},\gamma\vec{r}) = \frac{4\pi}{\gamma k_{aA}\gamma}\sum_{l_a\lambda_a} u_{l_a}(k_{aA},\gamma r) i^{l_a} Y_{l_a\lambda_a}(\hat{r}) Y^*_{l_a\lambda_a}(\hat{k}_{aA}) \ , \tag{32}$$

$$\chi^{(-)*}_{aB}(\vec{k}_{aB},\vec{r}) = \frac{4\pi}{k_{aB}\gamma}\sum_{l'_a\lambda'_a} u_{l'_a}(k_{aB},r) i^{-l'_a} Y_{l'_a\lambda'_a}(\hat{r}) Y^*_{l'_a\lambda'_a}(\hat{k}_{aB}) \ , \tag{33}$$

$$\chi^{(-)*}_{bB}(\vec{k}_{bB},\vec{r}) = \frac{4\pi}{k_{bB}\gamma}\sum_{l_b\lambda_b} u_{l_b}(k_{bB},r) i^{-l_b} Y_{l_b\lambda_b}(\hat{r}) Y^*_{l_b\lambda_b}(\hat{k}_{bB}) \ , \tag{34}$$

and write the "bound state" cluster wave function

$$\phi^{\alpha}_{L\Lambda}(\vec{r}) = R_{\alpha L}(r) i^L Y_{L\Lambda}(\hat{r}) \ . \tag{35}$$

After carrying out various angular integrations and choosing the $\vec{z}$ axis along $\vec{k}_{aA}$ and $\vec{y}$ axis along $k_{aA} \times k_{aB}$, we obtain finally

$$T^{\alpha L\Lambda}_{BA} = \frac{\sqrt{4\pi}}{\gamma k_{aA} k_{aB} k_{bB}} \sum_{l_a l'_a l_b \lambda_b kq} i^{l_a+L-l'_a-l_b} \frac{(2l_a+1)(2l'_a+1)(2l_b+1)}{(2k+1)}$$
$$\times (l_b\lambda_b L\Lambda|kq)(l_b 0 L 0|k0)(l_a 0 l'_a q|kq)(l_a 0 l'_a 0|k0)\ I^L_{l_a l'_a l_b} d^{l'_a}_{q0}(\theta_a) d^{l_b}_{\lambda_b 0}(\theta_b) e^{-i\lambda_b\phi_b} \ , \tag{36}$$

where the particles are detected at c.m. angles $(\theta_a, 0)$ and (θ_b, ϕ_b), respectively. The quantity $d^l_{mn}(\theta)$ is a reduced rotation matrix element and

$$I^L_{l_a l'_a l_b} = \int_0^\infty u_{l_a}(k_{aA},\gamma r) u_{l'_a}(k_{aB},r) u_{l_b}(k_{bB},r) R_{\alpha L}(r) dr/r \ . \tag{37}$$

Finally, we introduce fully relativistic expressions for the phase space and incident flux terms in Eq. (1). The result is

$$\frac{d^3\sigma^{LJ}}{d\Omega_a d\Omega_b dE_a} = C^2 |\langle\bar{t}\rangle|^2 S_{LJ} \left\{ \frac{E_a E'_a E_b}{(2\pi)^5(\hbar c)^7} \frac{P'_a P_b c}{P_a} \frac{1}{1+(E_b/E_B)[1-(P_a/P_b)\cos\theta_{ab}+(P'_a/P_b)\cos\theta_{a'b}]} \right\} \sum_\Lambda |T^{\alpha L\Lambda}_{BA}|^2 \ , \tag{38}$$

where c is the velocity of light, E_i is the relativistic total energy of particle i, and the c.m. angles are obtained using Eq. (28). It is this expression (with $C^2|\langle\bar{t}\rangle|^2 S_{LJ}$ set equal to unity) which is evaluated in the computer code WAVE used in the calculations which follow.

C. Summary of approximations

Before proceeding to a discussion of the numerical calculations it is convenient to summarize certain major approximations which we have employed in order to obtain the comparatively simple result given in Eq. (38).

Firstly, we have made the impulse approximation in replacing the exact t operator t_{BA} by the operator for the free scattering process $t^{(+)}_f$. It is possible to write down an expression for the error in the impulse approximation due to changes in the potentials during the two-body collision as well as an additional term largely representing multiple scattering effects.[16] Unfortunately, even in a simple three-body model, formal theoretical tests of the DWIA are rather involved.[17] However, for nucleon knockout on ^{4}He it appears that the DWIA tends to overestimate the exact cross section and that this problem becomes progressively less serious as the projectile energy is increased.[17]

Secondly, we have assumed factorization so that the matrix elements of $t^{(+)}_f$ may be taken outside the integration in T_{BA} and evaluated for the asymptotic particle momenta. Evidently this approximation requires that $t^{(+)}_f$ vary little with momentum and/or the momentum spreading arising from the distorting potentials is small, at least for the regions of configuration space which contribute strongly to the cross section.

Thirdly, the entrance channel distorting potential V_{aB} is, strictly, the optical potential for scattering from the core B averaged over the target A. Clearly such a potential cannot be obtained directly by fitting data from any real scattering experiment. In the following calculations we used potentials which reproduced $a+A$ scattering with both real and imaginary well depths reduced by a factor B/A.

Fourthly, we have omitted the term $T_{\rm coup}$ in Eq. (22) in order to obtain a simple product form for the three-body final state wave function. Other approaches are possible.[18] However, this so-called "kinetic energy approximation" does become exact in the limit as m_B tends to infinity. In addition, as pointed out by Jain *et al.*,[8] the approxima-

tion becomes exact in the plane-wave limit. In the present work the effect of T_{coup} on the asymptotic relative energies is correctly handled although any other effects it may have on the scattering wave functions are omitted. It is arguable that since T_{coup} involves a scalar product of momentum operators its effect will be greatly reduced with the c.m. opening angle between particles a' and b is close to 90°.

Our fifth major approximation is to project the target wave function not only onto the residual state B but also onto the emitted cluster ground state wave function. This corresponds to the assumption that it is only that part of the target wave function which looks like a "preformed" cluster b which contributes appreciably to the cross section. Since such clusters tend to be formed more readily in the nuclear surface region the validity of this approximation may well be correlated with the degree of surface localization of the reaction.

An additional approximation made in all of the following calculations is to replace the wave function of A projected onto $B+b$ by $\phi^{\alpha}_{LA}(\vec{r}_{bB})$, a wave function generated in a Woods-Saxon well. This procedure does correctly reproduce the appropriate $A \rightarrow B+b$ separation energy but may not fully take into account effects due to antisymmetrization between the groups B and b. To the extent that the oscillator shell model correctly reproduces the wave functions of A, B, and b the error may not be too serious, however. Thus N, the principle quantum number for $\phi^{\alpha}_{LA}(\vec{r}_{bB})$, is chosen by counting the available shell model oscillator quanta and assigning zero to b (usually a nucleus in the 1S shell) and the remainder to the relative motion of B and b.

Finally, it should be noted that in evaluating the spin-summed and averaged two-body t matrix $|\langle\bar{t}\rangle|^2$ we have neglected the fact that the struck cluster b is, in fact, off the mass shell. Instead, we have evaluated $|\langle\bar{t}\rangle|^2$ at a nearby on-shell point using an interpolation of available differential cross sections for free $a+b$ elastic scattering. This point is discussed further in Refs. 19 and 20.

III. RESULTS FOR $(p,p\alpha)$ REACTIONS

We next present systematic features which have emerged from our calculations and discuss the implications of these results for the $(p,p\alpha)$ analyses of Ref. 20 (which is referred to hereafter as II). It is, of course, no surprise that our results have much in common with earlier calculations for $(p,2p)$ reactions.

Firstly, we find that distortion effects are generally large. In Fig. 1 are shown typical results for 100 MeV $^{12}C(p,p\alpha)^{8}Be$(g.s.) data taken from II. This is an $L=0$ transition in which the α cluster is ejected from a 3S orbit. Optical potentials used in this calculation (and all others we shall consider) are listed in Table I. In the figure two curves are shown. The broken curve is a PWIA calculation which seriously underestimates the width of the distribution and also predicts a pronounced minimum which is not observed experimentally. These deficiencies are eliminated very nicely in the DWIA calculation which agrees very well with the data, apart from the region of high proton energy where sequential processes contribute significantly. We recall that, in the spirit of the PWIA, the distribution shown is essentially the square of the momentum wave function of the bound α cluster. Thus, had we neglected distortion effects, we would have erroneously concluded that the chosen α cluster wave function had insufficient high momentum components.

In Fig. 1 both curves were arbitrarily normalized to experiment. We note from Eq. (17) that the corresponding normalization factor is the cluster spectroscopic factor S_{LJ} defined in Eq. (16). In general, if distortion effects are omitted the $(p,p\alpha)$ cross section is overestimated and hence the extracted value of S_{LJ} is too small. For the data of Fig. 1 the PWIA result for S_{LJ} is roughly 10 times smaller than the DWIA result. Similar behavior is found for other targets. In Fig. 2 is shown the energy variation of the ratio of the cross section for reaction $^{24}Mg(p,p\alpha)^{20}Ne$ (g.s.) calculated in DWIA to the same quantity calculated in PWIA. The detected proton angle is 60° and the detected α particle angle and energy are chosen so that the residual nucleus is at rest. One sees that at 50 MeV a plane-wave calculation would be in error by more than 3 orders of magnitude, while even at 250 MeV the error is roughly a fac-

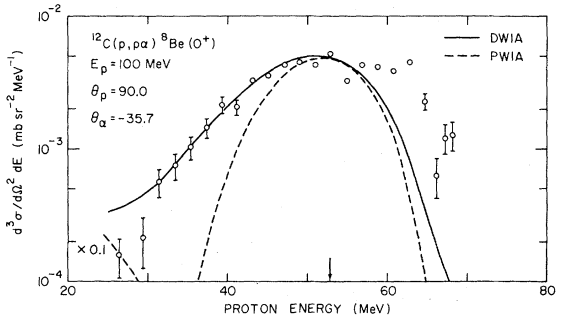

FIG. 1. Energy sharing results for the ^{12}C-$(p,p\alpha)^{8}Be$(g.s.) reaction at $E_0=100$ MeV, $\theta_p=90.0°$, and $\theta_\alpha=-35.65°$. The data are from Ref. 20. The solid curve is a DWIA calculation, and the dashed curve is a PWIA calculation. Both calculations are normalized to the data.

TABLE I. Optical potential parameters used. The optical potential is defined to be:

$$V_{\text{opt}}(r) = -Vf(r, r_0, a) - i\left(W - 4W_D a' \frac{d}{dr}\right) \times f(r, r_0', a') + V_{\text{Coulomb}},$$

where

$$f(r, r_0, a) = \left[1 + \exp\left(\frac{r - r_0 A^{1/3}}{a}\right)\right]^{-1};$$

A is the target mass and V_{Coulomb} is the Coulomb potential of a uniform sphere of charge of radius $r_c A^{1/3}$.

Reaction	System	V	r_0	a	r_c	W	W_D	r_0'	a'	Ref.
$^{12}C(p,p\alpha)^{8}Be$(g.s.)	$p + {}^{12}C$	21.2	1.33	0.65	1.33	6.5	0.0	1.46	0.44	20
$E_0 = 100$ MeV	$p + {}^{8}Be$	32.3	1.26	0.63	1.30	0	2.3	1.31	0.96	20
	$\alpha + {}^{8}Be$	88.9	0.99	0.31	1.20	4.9	0.0	3.01	0.58	20
	Bound state	89.9	1.24	0.78	1.24					
$^{24}Mg(p,p\alpha)^{20}Ne$(g.s.)	$p + {}^{24}Mg$	38.0–0.0[a]	1.43	0.62	1.30	12.0–17.0[a]	0.0	1.15	0.63	21
$E_0 = 50$–350 MeV	$p + {}^{20}Ne$	43.0–2.3[a]	1.43	0.62	1.30	10.0–16.0[a]	0.0	1.15	0.63	21
	$\alpha + {}^{20}Ne$	92.0	1.40	0.709	1.40	47.9	0.0	1.40	0.709	24
	Bound state	125.5	1.24	0.78	1.24					
$^{20}Ne(\alpha,2\alpha)^{16}O$(g.s.)	$\alpha + {}^{20}Ne$	92.0	1.40	0.709	1.40	47.9	0.0	1.40	0.709	24
$E_0 = 78$ MeV	$\alpha + {}^{16}O$	92.0	1.40	0.709	1.40	47.9	0.0	1.40	0.709	24
[Set (a)]	Bound state	125.5	1.24	0.78	1.24					
$^{20}Ne(\alpha,2\alpha)^{16}O$(g.s.)	$\alpha + {}^{20}Ne$	151.6	1.39	0.62	1.40	33.9	0.0	1.39	0.62	24
$E_0 = 78$ MeV	$\alpha + {}^{16}O$	151.6	1.39	0.62	1.40	33.9	0.0	1.39	0.62	24
[Set (b)]	Bound state	125.5	1.24	0.78	1.24					
$^{16}O(\alpha,2\alpha)^{12}C$(g.s.)	$\alpha + {}^{16}O$	120.0	1.29	0.754	1.30	47.9	0.0	1.40	0.709	24
$E_0 = 90$ MeV	$\alpha + {}^{12}C$	120.0	1.29	0.754	1.30	47.9	0.0	1.40	0.709	24
	Bound state	72.48	1.24	0.78	1.24					

[a] Range of well depths used for the minimum to maximum energies.

tor of 10. Of interest is the fact that, contrary to a popular argument, the calculated cross section does not approach the plane-wave limit at higher energies. Indeed, from the point of view of minimizing distortion effects, there appears to be no significant advantage in incident energies in excess of 150 MeV. Thus, since a proper treatment of distortion effects cannot be avoided, our chosen incident energy of 100 MeV appears to be quite suitable, particularly in view of the greater experimental difficulty of the higher energy experiments.

In the calculations shown in Fig. 2 proton optical potentials used were based upon the analysis of 155 MeV proton scattering by Comparat *et al.*[21] The strength of the real well depth V was assumed to vary with incident energy E according to $V = V_{155} - \alpha(E - 155)$, where $\alpha = 0.25$ for $E < 155$ MeV and $\alpha = 0.1$ for $E > 155$ MeV. For the imaginary well depth we assumed $W = W_{155} + 0.02(E - 155)$. These expressions lead to results quite similar to the energy dependence found by van Oers[22] as well as results reported by Igo.[23] For the emitted α particle we used the potential obtained by Singh *et al.*[24] for elastic α particle scattering from ^{24}Mg at 80 MeV. No energy variation of the param-

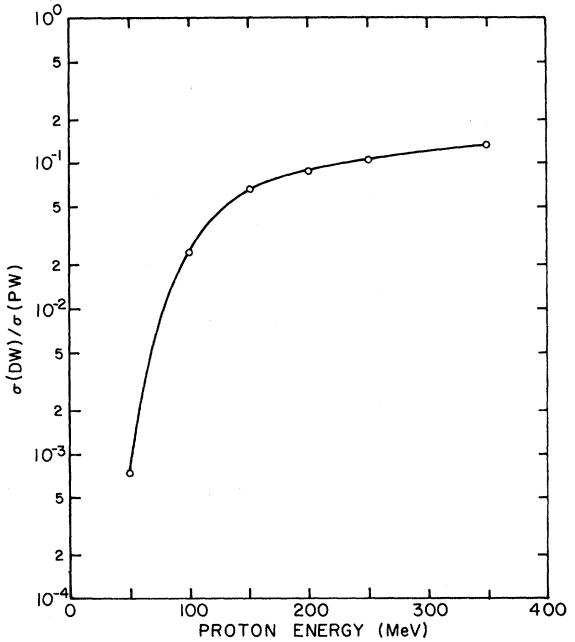

FIG. 2. Ratio of the cross section for ^{24}Mg-$(p,p\alpha)^{20}Ne$(g.s.) calculated in DWIA to that calculated in PWIA as a function of proton bombarding energy. The proton is detected at 60° (lab). The α particle angle and both detected energies are chosen so that the residual nucleus is left at rest.

eters was included. Using the results of Ref. 23, we estimate that, over the range of α particle energies involved, both real and imaginary well depths are likely to be constant to within $\pm 5\%$. Such a variation would not qualitatively change the results of Fig. 2.

A second systematic feature of our calculations is the fact that the quasifree $(p,p\alpha)$ reaction is usually quite strongly surface localized. This is a consequence not only of the pronounced distortion effects but also of the choice of experimental geometry which permits exact momentum and angular momentum matching. As discussed in II, the degree of surface localization directly influences the validity of the factorization approximation. In addition, as is well known, it is in the nuclear surface that our decision to retain only the α-particlelike component of the target wave function has greatest validity.

In Fig. 3 surface localization effects are shown for the ^{24}Mg$(p,p\alpha)^{20}$Ne(g.s.) reaction at incident proton energies between 50 and 350 MeV. The kinematic conditions and optical potentials were chosen to be identical to those chosen for the calculations of Fig. 2. Thus the residual nucleus has zero recoil momentum. Plotted are histograms of contributions to the DWIA cross section obtained by taking differences between calculations with different lower radial cutoffs. Also shown is the $5S$ bound α cluster radial wave function used in the calculation, the proton density distribution[25] for ^{24}Mg, and a histrogram of contributions to a PWIA calculation at 100 MeV. It should be noted that PWIA calculations for the other energies differ only in absolute magnitude. As expected, the PWIA result is quite similar in shape to the $5S$ bound state wave function. In contrast, for the DWIA calculations the reaction is more strongly surface localized. For the higher energies the main contributions to the $(p,p\alpha)$ cross section result from roughly the 3% density region. At 50 MeV (where the overall absolute cross section is much reduced) a significant contribution from smaller radii is apparent. That this contribution interferes destructively with the surface contribution is a consequence of phasing difficulties resulting from the optical potentials rather than sign changes in the radial wave function. This effect is much reduced at 100 MeV and disappears entirely at 155 MeV and above. Results of analogous calculations for ^{12}C$(p,p\alpha)^{8}$Be(g.s.) are qualitatively the same. Finally, it is worth noting that DWIA calculations for nonzero values of the residual nucleus recoil momentum are still dominated by the surface region, although the results do indicate somewhat greater contributions from the nuclear interior.

IV. RESULTS FOR $(\alpha,2\alpha)$ REACTIONS

α particle clustering may also be studied by $(\alpha,2\alpha)$ reactions. At energies close to 100 MeV this is an attractive alternative to $(p,p\alpha)$ studies since certain experimental difficulties are alleviated. In addition, DWIA calculations suggest that

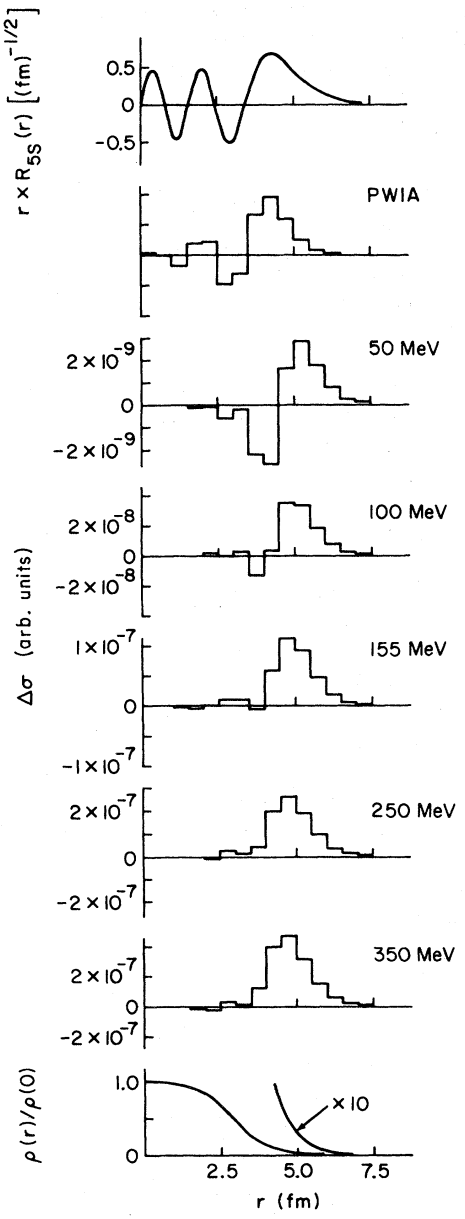

FIG. 3. Radial distributions of contributions $\Delta\sigma$ to the DWIA cross section for ^{24}Mg$(p,p\alpha)^{20}$Ne(g.s.) for the results presented in Fig. 2. Also presented are the radial contributions to the PWIA cross section (identical shape at all energies), the $5S$ α single-particle wave function, and the nuclear charge distribution $\rho(r)/\rho(0)$ taken from electron scattering results.

the $(\alpha,2\alpha)$ reaction will exhibit even more pronounced surface localization than $(p,p\alpha)$. For example, in Fig. 4 contributions to the DWIA cross section for ^{20}Ne$(\alpha,2\alpha)^{16}$O(g.s.) are plotted as a function of radius. The incident energy is 78 MeV and the α particles are detected at equal angles and energies so that the residual nucleus recoil momentum is zero. Also shown is the bound α cluster wave function. One observes the essentially all the yield comes from the asymptotic portion of the wave function. Comparing these results with the ^{24}Mg$(p,p\alpha)^{20}$Ne(g.s.) calculations shown in Fig. 3, we see that the yield curve is pushed out by about 2 fm, indicating much stronger absorption. Clearly the $(\alpha,2\alpha)$ reaction takes place in regions of very low nuclear density. Thus the factorization approximation should be more reliable than for $(p,p\alpha)$, and the correct treatment of the bound α cluster wave function will be a critical ingredient in any analysis of $(\alpha,2\alpha)$ data.

Unfortunately, difficulties are encountered in DWIA analyses for $(\alpha,2\alpha)$ reactions at these energies which are not apparent in our $(p,p\alpha)$ studies. For example, in Fig. 5 we show a DWIA calculation for the 78 MeV ^{20}Ne$(\alpha,2\alpha)^{16}$O(g.s.) data of Epstein *et al.*[26] The optical potentials used for the calculations of Figs. 4 and 5 were taken from the analysis by Singh *et al.*[24] of 40 and 80 MeV α elastic scattering on ^{24}Mg and are listed as Set (a) in Table I. The α particle bound state wave function was obtained by binding an α particle in a 5*S* orbit in a Woods-Saxon well with the parameters listed in Table I. In Fig. 5 it is seen that agreement between the DWIA calculation and experiment is quite disappointing. This is in marked contrast to all $(p,p\alpha)$ calculations we have carried out to date.[20,27] Calculations using a deeper family optical potential[24] in both entrance and exit channels [Set (b) in Table I] predicted an energy sharing distribution essentially identical in shape to the curve shown in Fig. 5. and differed by only 10% in magnitude. That the predictions are even less sensitive to the choice of optical potentials than calculations for $(p,p\alpha)$ reactions is presumably a consequence of the extreme surface localization in $(\alpha,2\alpha)$ which results in dominance of high partial waves. It is the surface and higher partial waves which are essentially the same for different optical potential families.

On normalizing the DWIA curve of Fig. 5 to experiment an α cluster spectroscopic factor of about 12 is obtained. This value seems unreasonably large and cannot be reduced significantly by reasonable optical parameter and bound state parameter variation. It is to be compared with an experimental value of $S_\alpha \sim 0.3$ obtained in studies[27,28] of ^{24}Mg$(p,p\alpha)^{20}$Ne(g.s.) and theoretical values[28,29] of 0.08 and 0.23 for ground state to ground state α cluster removal from ^{24}Mg and ^{20}Ne, respectively. A more reasonable result can be obtained using a PWIA calculation with a Hulthén bound state wave function and a lower radial cutoff.[26] We feel that this has no great theoretical significance.

Similar problems are encountered in the ^{16}O$(\alpha,2\alpha)^{12}$C experiment using 90 MeV incident α particles.[30] In Ref. 30 Sherman and Hendrie are

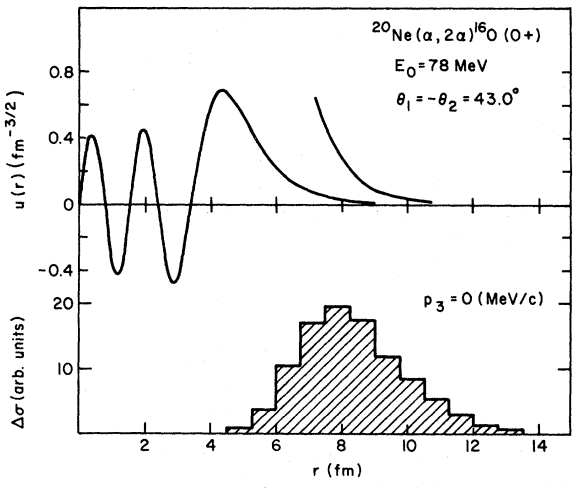

FIG. 4. Radial distribution of contributions $\Delta\sigma$ to the DWIA cross section for ^{20}Ne$(\alpha,2\alpha)^{16}$O(g.s.) at E_α =78 MeV. The kinematic conditions are chosen so that the residual nucleus is left at rest. Also shown is the 5*S* α single-particle wave function.

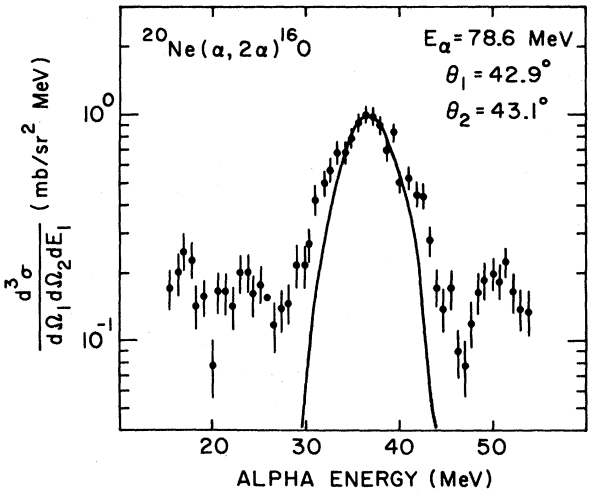

FIG. 5. Energy sharing results for the ^{20}Ne-$(\alpha,2\alpha)^{16}$O(g.s.) reaction at E_α =78 MeV, $\theta_{\alpha1}$ =42.9°, and $\theta_{\alpha2}$ =43.1°. The data are from Ref. 26. The solid curve is a DWIA calculation.

able to reproduce their data quite well using a DWIA calculation employing a parametrized approximation to the distorted waves. Unfortunately, their result may be misleading since an exact treatment of distortion effects does not reproduce the approximate results. In Fig. 6 we show our DWIA predictions for $^{16}O(\alpha,2\alpha)^{12}C$ at 90 MeV together with data from Ref. 30. Optical parameters used are taken from the analysis of Singh *et al.*[24] of elastic α particle scattering from ^{24}Mg. For the gound state transition the α cluster was removed from a $3S$ orbit with the parameters listed in Table I. For the excited state a $2D$ configuration was assumed. For the ground state transition the width of the experimental distribution is underestimated and, for the excited state transition, the data is again poorly described by the calculation. It is interesting to note for the excited state transition, that the minimum at zero recoil momentum expected in PWIA for an $L=2$ transition, is totally obscured as a result of the large distortion effects.

As we have pointed out elsewhere, if the poor agreement in shape between theory and experiment is ignored the normalization factors for the two curves may be used to estimate spectroscopic

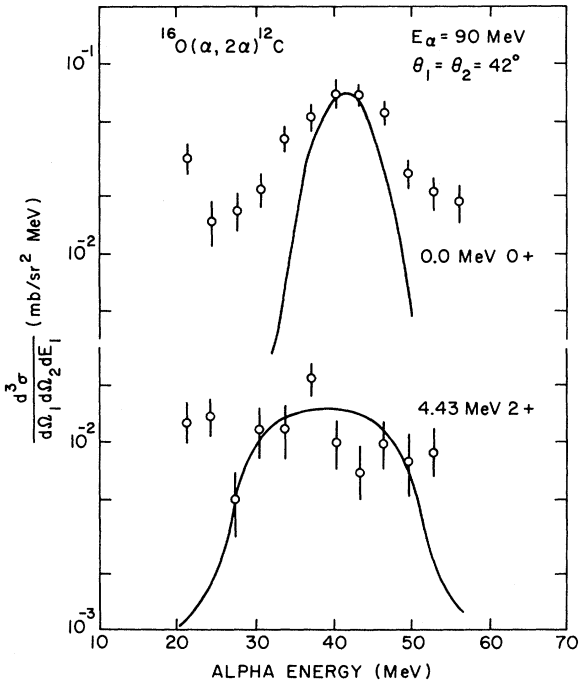

FIG. 6. Energy sharing results for the $^{16}O(\alpha,2\alpha)^{12}C$ ground state (0+) and 4.43 MeV state (2+) reactions at $E_\alpha = 90$ MeV, and $\theta_{\alpha 1} = -\theta_{\alpha 2} = 42°$. The data are from Ref. 30. The solid curves are DWIA calculations normalized to the data.

factors. As a result[27] the value of S_{2+}/S_{0+}, the spectroscopic factor for the excited state relative to the ground state, rises from 0.24, the PWIA estimate obtained in Ref. 30, to ~8 in our DWIA analysis. This is to be compared with a shell model prediction[13] of 5.7. Thus, provided distortion effects are considered, the observed strength of the 2+ state in the $(\alpha,2\alpha)$ experiment is more than sufficient to establish this level as the principal parent of the ^{16}O ground state in agreement with theory[13] and transfer experiments.[31]

Unfortunately, to ignore the poor agreement in shape between theory and experiment has little merit. For the ground state transition the discrepancy is quite similar to that found in our $^{20}Ne(\alpha,2\alpha)^{16}O$(g.s.) calculations shown in Fig. 5. Furthermore, for the $^{16}O(\alpha,2\alpha)^{12}C$(g.s.) case we obtain $S_{0+} \sim 15$, a value quite similar to that obtained for $^{20}Ne(\alpha,2\alpha)^{16}O$(g.s.). We emphasize again that we have not encountered corresponding problems in our $(p,p\alpha)$ analyses.

Values of S_{0+} for $^{16}O(\alpha,2\alpha)^{12}C$ are listed in Table II for the 90 MeV experiment together with the shell model prediction[13] and experimental values extracted from our DWIA analyses[27] of the data[32] at 52.5 MeV and the data[33] at 850 MeV. The extracted value for S_{0+} of ~15 obtained at 90 MeV is to be compared with the theoretical value of 0.23. Thus, taking the shell model calculation as a reasonable estimate of the correct spectroscopic factor, the DWIA underestimates the 90 MeV cross section by ~65. From Table II we see that at 52.5 MeV the problem is roughly 10 times worse. On the other hand, at 850 MeV our DWIA analysis of data including all final states below 30 MeV excitation yields an upper limit of ~1.8 which, we argue, represents quite satisfactory agreement with theory. Thus, at 850 MeV the DWIA appears to be successful in predicting the $^{16}O(\alpha,2\alpha)^{12}C$ absolute cross section.

In an attempt to understand this phenomenon we also include in Table II the ratio of the PWIA and DWIA predictions at the zero recoil momentum point of each energy sharing distribution. Only for the 850 MeV calculation is the value (of 5.4) similar to ratios encountered in our $(p,p\alpha)$

TABLE II. Ground state spectroscopic factor for $^{16}O(\alpha,2\alpha)^{12}C$.

E_α	S_{0+}	σ_{PW}/σ_{DW}
Theory	0.23	
850 MeV	<1.8	5.4
90 MeV	15	~1500
52.5 MeV	150	~3200

analyses which typically are between ~2 and ~20. For the 90 MeV calculation the ratio is 1500 while the value at 52.5 MeV is 3200. Clearly, at the lower energies, the first order diagram on which our ideas are largely based is almost completely cancelled by that class of higher order diagrams which are approximated by the DWIA. In this situation we argue that it is probably necessary to introduce other classes of diagrams and hence the failure of the DWIA is no surprise. Consistent with this notion is the result that the corresponding ratios for other reactions which are successfully described by distorted-wave Born-approximation theory are typically one to two orders of magnitude smaller than the 52.5 and 90 MeV $(\alpha, 2\alpha)$ results. For example, for (d,p) and (p,d) reactions plane-wave/distorted-wave ratios at energies above the Coulomb barrier are typically[34] ~10 and may rise to ~60 in some cases.[35]

Finally, it is worth noting that agreement in absolute cross section for the 90 MeV $(\alpha, 2\alpha)$ experiment could be obtained by adjusting the bound state well parameters so as to increase the resultant wave function in the asymptotic region by ~8. (Reasonable variations in distorting parameters do not alleviate the problem significantly.) We argue that the resulting parameters ($r_0 = 2.35$ fm, $a = 0.78$ fm) are unphysical. In addition, we point out that no improvement in the shapes of the calculated curves would result and that the corresponding decrease in S_{0^+} for the 850 MeV data would pose difficult problems of interpretation.

V. SUMMARY AND CONCLUSIONS

The formalism for a simple factorized distorted-wave impulse-approximation calculation for quasi-free cluster knockout has been outlined. Calculations for $(p,p\alpha)$ and $(\alpha, 2\alpha)$ reactions have been presented.

For both reactions distortion effects are found to be large and analysis of data using the PWIA must lead to serious error. Not only will spectroscopic factors extracted using PWIA be underestimated, but also the interpretation of energy sharing data in terms of the struck-particle momentum distribution is potentially misleading. In general, both reactions are quite strongly surface localized and hence show sensitivity to the magnitude of the cluster wave function in the nuclear surface. This is much the same information which is obtained in analyses of cluster transfer experiments.

A DWIA calculation for $^{12}C(p,p\alpha)^8Be$(g.s.) at 100 MeV showed that, despite strong surface localization, the introduction of distortion effects increased the width of the energy sharing distribution. This effect is also found in the DWIA calculations for $(p,p\alpha)$ reactions in II. It cannot be reproduced in PWIA by using a lower radial cutoff.

A study of the energy dependence of distortion effects for $^{24}Mg(p,p\alpha)^{20}Ng$(g.s.) suggested that 100 MeV, the energy employed in II, is suitable in order to avoid large distortion effects, and that there is no significant gain beyond 200 MeV.

Analyses of $(\alpha, 2\alpha)$ reactions on ^{16}O and ^{20}Ne targets at energies up to 90 MeV produced quite poor agreement with experiment both in shape and magnitude. This behavior, quite unlike $(p,p\alpha)$ analyses at 100 MeV, may be correlated with much larger distortion effects encountered in the $(\alpha, 2\alpha)$ calculations. Thus, other omitted diagrams may contribute significantly to the $(\alpha, 2\alpha)$ cross section. At 850 MeV, where distortion effects are more similar to $(p,p\alpha)$, there is no evidence that the difficulties encountered in the lower energy $(\alpha, 2\alpha)$ analyses persist.

In conclusion we argue that the $(p,p\alpha)$ reaction in conjunction with the DWIA should prove to be a useful spectroscopic tool most conveniently studied at incident energies of 100–200 MeV. In the case of $(\alpha, 2\alpha)$ reactions spectroscopic studies probably should employ significantly higher energies where, unfortunately, technical difficulties are more severe. On the other hand, interesting reaction mechanism problems are posed by this reaction and a careful study of energy dependence is called for with $(\alpha, 2\alpha)$ data at incident energies in excess of 90 MeV being most desirable.

ACKNOWLEDGMENTS

We are indebted to Dr. E. F. Redish for assistance and to our other colleagues at Maryland for many stimulating discussions. Calculations were carried out using the UNIVAC 1108 of the Computer Science Center of the University of Maryland. Their generous provision of computer time is gratefully acknowledged. Finally, we are indebted to Thomas W. White who patiently initiated us into many mysteries of the UNIVAC system.

---

*Work supported in part by the U.S.E.R.D.A.

[1]See, e.g., M. Riou, Rev. Mod. Phys. 37, 375 (1965); B. Gottschalk and S. L. Kannenberg, Phys. Rev. C 2, 24 (1970); D. Bachelier *et al.*, Phys. Rev. C 7, 165 (1973); P. G. Roos and N. S. Chant, *Proceedings of the Second International Conference on Clustering Phenomena in Nuclei, College Park, 1975*, edited by D. A. Goldberg, J. B. Marion, and S. J. Wallace (ERDA

Technical Information Center, Oak Ridge, Tennessee), p. 242; P. G. Roos *et al.*, Phys. Rev. C 15, 69 (1977). following paper; N. S. Chant and P. G. Roos, *Proceeding of the Second International Conference on Clustering Phenomena in Nuclei, College Park, 1975* (see above), p. 265; D. Bachelier *et al.*, Nucl. Phys. A268, 488 (1976).

[2]See, e.g., G. Audi, C. Detraz, M. Langevin, F. Poughеon, Nucl. Phys. A237, 300 (1975); N. Anantaraman *et al.*, Phys. Rev. Lett. 35, 1131 (1975); F. D. Becchetti, L. T. Chua, J. Jänecke, A. M. Van der Molen, Phys. Rev. Lett. 34, 225 (1975); W. F. Steele, P. A. Smith, J. E. Finck, and G. M. Crawley, Report No. MSUCL 186, 1975 (unpublished).

[3]See, e.g., R. M. DeVries, Phys. Rev. C 8, 951 (1973); R. M. DeVries, Phys. Rev. Lett. 30, 666 (1973).

[4]D. F. Jackson and T. Berggren, Nucl. Phys. 62, 355 (1965).

[5]K. L. Lim and I. E. McCarthy, Phys. Rev. 133, B1006 (1964); Phys. Rev. Lett. 13, 446 (1964).

[6]B. K. Jain and D. F. Jackson, Nucl. Phys. A99, 113 (1967).

[7]A. K. Jain, N. Sarma, and B. Banerjee, Nucl. Phys. A142, 330 (1970).

[8]A. K. Jain *et al.*, Nucl. Phys. A216, 519 (1973).

[9]L. S. Rodberg and Roy M. Thaler, *Introduction to the Quantum Theory of Scattering* (Academic, New York and London, 1967), Chap. 7.

[10]I. S. Shapiro, V. M. Kolybasov, and G. R. Augst, Nucl. Phys. 61, 353 (1965).

[11]M. H. MacFarlane and J. B. French, Rev. Mod. Phys. 32, 567 (1960).

[12]M. Ichimura, A. Arima, E. C. Halbert, and T. Teresawa, Nucl. Phys. A204, 225 (1973).

[13]D. Kurath, Phys. Rev. C 7, 139 (1973).

[14]N. Anyas-Weiss *et al.*, Phys. Rep. 12C, 203 (1974).

[15]R. D. Koshel, Nucl. Phys. A260, 401 (1976).

[16]J. S. Blair and E. M. Henley, Phys. Rev. 112, 2029 (1958).

[17]S. K. Young and E. F. Redish, Phys. Rev. C 10, 498 (1974).

[18]D. F. Jackson, Nucl. Phys. A90, 209 (1967).

[19]See Roos and Chant (Ref. 1), p. 242.

[20]See Roos *et al.* (Ref. 1), referred to as II.

[21]V. Comparat *et al.*, Nucl. Phys. A221, 403 (1974).

[22]W. T. H. van Oers and H. Haw, Phys. Lett. 45B, 227 (1973); W. T. H. van Oers, Phys. Rev. C 3, 1550 (1971).

[23]G. Igo (private communication).

[24]P. P. Singh, R. E. Malmin, M. High, and D. W. Devins, Phys. Rev. Lett. 23, 1124 (1969).

[25]L. R. B. Elton, *Nuclear Sizes* (Oxford U.P., London, 1961), Chap. 2.

[26]M. B. Epstein, D. J. Margaziotis, N. S. P. King, and T. A. Cahill, Phys. Rev. C 9, 581 (1974).

[27]See Chant and Roos (Ref. 1), p. 265.

[28]See Bachelier *et al.* (Ref. 1).

[29]J. D. Cossairt *et al.*, Nucl. Phys. A261, 373 (1976).

[30]J. D. Sherman, D. L. Hendrie, and M. S. Zisman, Phys. Rev. C 13, 20 (1976).

[31]G. J. Wozniak, N. A. Jelley, and J. Cerny, Phys. Rev. Lett. 31, 607 (1973).

[32]A. Guichard *et al.*, Phys. Rev. C 4, 700 (1971).

[33]N. Chirapatpimol *et al.*, Nucl. Phys. A264, 379 (1976).

[34]N. K. Glendenning, Annu. Rev. Nucl. Sci. 13, 191 (1963).

[35]P. G. Roos (private communication); P. G. Roos *et al.*, Nucl. Phys. A255, 187 (1975).